How to Cite
Adnyana, I. G. A. P., Sukarasa, I. K., & Suarbawa, K. N. (2021). Synthesis and characterization of permanent magnetic oxide system Ba1-x-yLaxCeyFe12O19 system doped with La-Ce metal using wet mechanical milling method. *International Journal of Chemical & Material Sciences*, *4*(1), 43-48. https://doi.org/10.21744/ijcms.v4n1.1797

Synthesis and Characterization of Permanent Magnetic Oxide System $Ba_{1-x-y}La_xCe_yFe_{12}O_{19}$ System Doped with La-Ce Metal Using Wet Mechanical Milling Method

I Gusti Agung Putra Adnyana
Program of Physics study, Department of Physics, Faculty of Mathematics and Natural Sciences, Udayana University, Denpasar, Indonesia
Corresponding author email: igaadnyana@unud.ac.id

I Ketut Sukarasa
Program of Physics study, Department of Physics, Faculty of Mathematics and Natural Sciences, Udayana University, Denpasar, Indonesia

Komang Ngurah Suarbawa
Program of Physics study, Department of Physics, Faculty of Mathematics and Natural Sciences, Udayana University, Denpasar, Indonesia

Abstract---The development of permanent magnet-based rare earth metals becomes a serious problem if the raw materials are difficult to find. The solution chosen is to utilize an oxide-based permanent magnet with little substitution of rare earth metals. This study presented a permanent magnetic synthesis of barium hexaferrite-based oxides that were doped with La and Ce atoms. The synthesis of this material uses the wet mechanical milling technique to obtain the single-phase permanent magnet system $Ba_{1-x-y}La_xCe_yFe_{12}O_{19}$ (x = 0, 0.02, 0.04 and y = 0. 0.05, 0.1). The precursor is weighed according to stoichiometric composition and is milled for 5 hours then compressed at a pressure of 7000 Psi. Sintering temperature for the formation of the barium hexaferrite phase at 1200^{o}C for 2 hours. All samples after sintering were characterized using XRD and EDS. A single-phase is obtained on all sample compositions with a hexagonal P63/mmc structure and is supported by elemental analysis data that each substituted sample contains elements La and Ce. Lattice parameters a, b, and c appear to decrease with increasing concentrations of La and Ce doping ions with a ratio of c/a in the range of 3.93-3.94.
Keywords---*Barium hexaferrite, crystal structure, mechanical milling, particle morphology, substitution of La and Ce.*

Introduction

A hard magnet or better known as a permanent magnet is an important component needed by the automotive industry because of no less than 200 components in a car consist of an electric motor. The electric motor needed in a car does not have to be very strong but must have a good temperature, corrosion, and demagnetization resistance. Permanent magnets on electric motors must be able to operate their performance at 200^{o}C without compromising their magnetic behavior (El Shater et al., 2018). There are two types of permanent magnets when viewed from their forming materials, namely permanent magnets of metal alloys and ceramic oxides. Both have their disadvantages and advantages. Permanent magnets based on metal alloys such as $Nd_2Fe_{14}B$ and SmCo5 are strong magnets but this type of magnetic manufacturing process is not easy, does not withstand corrosion, and the performance temperature is relatively low (Tc = 300^{o}C), in contrast to ceramic oxide-based permanent magnets i.e. hexagonal ferrite type-M ($XFe_{12}O_{19}$) where X is cationic divalent Ba or Sr, in addition to the manufacturing process is easy, it is corrosion-resistant, and the performance temperature is very high (Tc = 700^{o}C), but this type of oxide magnet has low product

ISSN 2632-9468
Submitted: 27 October 2021 |Revised: 18 November 2021 | Accepted: 09 December 2021

energy. Through material engineering and particle geometry, the energy of its products can be increased. Basically for some applications as an automotive drive electric motor not all require very strong magnets.

On the other hand, the presence of rare earth metals as mineral resources is increasingly difficult to find and is almost monopolized by some developed countries in the process of purification. However, this rare earth metal mineral has been found in the form of monazite sand in Indonesia although the deposits are not much and the purification process can already be mastered. The extraction of monazite sand can only produce lanthanum oxide (La_2O_3), cerium oxide (CeO_2), and neodymium oxide concentrate (Nd2O3). Based on extraction results from the potential of existing natural resources, it can be used for material engineering in the manufacture of M-type hexagonal-based magnets.

The ratio of magnet permanently based metal alloy ($Nd_2Fe_{14}B$) with ceramic oxide (hard ferrite) in terms of market number is 2: 1, while in terms of price is in a ratio of 25:1 (Bahadur et al., 2017). The combination of the two provides an opportunity for new magnets with energy products of 100–200 kJm^{-3}, which sits between hard ferrites (< 38 kJm^{-3}) and $Nd_2Fe_{14}B$ (> 200 kJm^{-3}) keeping in mind the cost of raw materials and processes that remain low (Bahadur et al., 2017). Some literature suggests that lanthanum substituted elements strontium and cobalt substitution of iron have been able to significantly improve the coercivity and magnetization field of remanent in the hexagonal ferrite (Adnyana et al., 2019; Adnyana et al., 2020; Vinnik et al., 2018). In addition, a reduction in particle size can also increase the coercivity field by almost twice if the particle size is less than 100 nm (Haritsah et al., 2019). Nevertheless, this reduction in particle size makes it a single domain, resulting in a strong dipolar force as opposed to its magnetic spin orientation under an external magnetic field (Nonaka et al., 2000). Because it is not easy to get anisotropic magnets from magnetic particles with a single domain, it is necessary to find a solution to be able to optimally obtain this coercivity field by going through the concept of doping with rare earth metal elements (Li et al., 2007).

Previous studies have been conducted in the manufacture of permanent oxide magnets substituted with La^{3+} ions. The result obtained is that a sample of barium hexaferrite doping ions La3+ was able to increase the magnetic coercivity field of this material with the best product energy found at the composition x = 0.04 with stoichiometric composition $Ba_{0.96}La_{0,04}Fe_{12}O_{19}$ (Adnyana et al., 2019). In addition, according to S. V. Trukhanov, that the increase in coercivity field is caused by magneto-crystalline energy or anisotropy field energy of this system material is increased. Subsequent research has been conducted on the synthesis and characterization of permanent magnetic materials based on barium hexaferrite yang doping Ce4+ ions. Phase identification results show that a single phase of the barium hexaferrite phase in the $Ba_{1-x}Ce_xFe_{12}O_{19}$ system is obtained at the composition x = 0.1, while for the composition of x > 0.1 has been formed a secondary phase. This can be explained by the energy magneto crystalline or energy anisotropy and the total number of moments in the dipole magnet (Adnyana et al., 2020).

This paper is focused on the synthesis process of barium hexaferrite type M with the substitution of La^{3+} ions and tetravalent ions Ce^{4+}. This is a unique new combination in which the La and Ce ions are expected to be able to partially replace the position of barium without interfering with the Fe position (Mosleh et al., 2014). The method used in prequel preparation is wet mechanical milling, which is expected to have advantages in its easy, simple, and inexpensive production process (Xu et al., 2006). In addition, this method in addition to reducing the particle size of the precursor is also able to make the mixture more homogeneous in a relatively short milling time (Song et al., 2008). To this end, in this study, researchers investigated the structure of barium hexaferrite anisotropic, with its chemical composition $Ba_{1-x-y}La_xCe_yFe_{12}O_{19}$ (Rezlescu et al., 1999).

Materials and Experiments

In this study, barium hexaferrite were doped to La^{3+} and Ce^{4+} ions with stoichiometric composition $Ba_{1-x-y}La_xCe_yFe_{12}O_{19}$ using variations in doping ion concentrations (x= 0; 0.02; 0.04 and y = 0; 0.05; 0.1). The method used is the wet mechanical milling method using oxide raw materials in the form of $BaCO_3$, Fe_2O_3, La_2O_3, and CeO_2 which all come from products with a high purity of 99.9%. Stoichiometric calculations for substitution variations La^{3+} and Ce^{4+} follow the reaction equation:

$$(1\text{-}x\text{-}y)BaCO_3 + xLa_2O_3 + yCeO_2 + 6Fe_2O_3 \rightarrow Ba_{1-x-y}La_xCe_yFe_{12}O_{19} + (1\text{-}x\text{-}y)CO_2$$

Each mixed composition is eroded using high-energy milling (PW1000 in mixer/mill) with several steel balls averaging 12 mm in diameter and a milling speed of 1000 rpm. Milling conditions include a ratio of ball weight to powder of 2:1, milling time for 5 hours, then compressed with a pressure of 7000 Psi, and sintering at a temperature of 1200ºC for 2 hours. A phase analysis both qualitatively and quantitatively for each sample that doped ions La^{3+}

and Ce^{4+} was studied using X-ray diffraction (XRD PANalytical XPert Pro). XRD measurements use Cu anode (λKα = 1.5406Å), step size 0.0263 and analyzed with GSAS software. As supporting data in XRD analysis, elemental analysis testing is conducted using energy dispersive spectroscopy (EDS JEOL JED 305).

Results and Discussions

The X-ray diffraction pattern of sample powders $Ba_{1-x-y}La_xCe_yFe_{12}O_{19}$ (x = 0, 0.02, 0.04 and y = 0, 0.05, 0.1) using CuKa anodes (l = 1.5406 A) and step sizes 0.0263 shown in figure. 1. The pure XRD pattern for $BaFe_{12}O_{19}$ (x = 0 and y = 0) has corresponded to the peak of the JCPDS data Bragg diffraction peak (card numbers 39-1433). Based on the JCPDS data, qualitative analysis can be shown that Bragg diffraction peaks of the samples XRD pattern with the composition x = 0.02, 0.04 and y = 0.05, 0.1 have the same profile with a relatively decreased intensity along with the increasing composition of x and y. Thus, according to qualitative analysis data shows that all samples It is a single phase with a hexagonal structure of P 63/mmc.

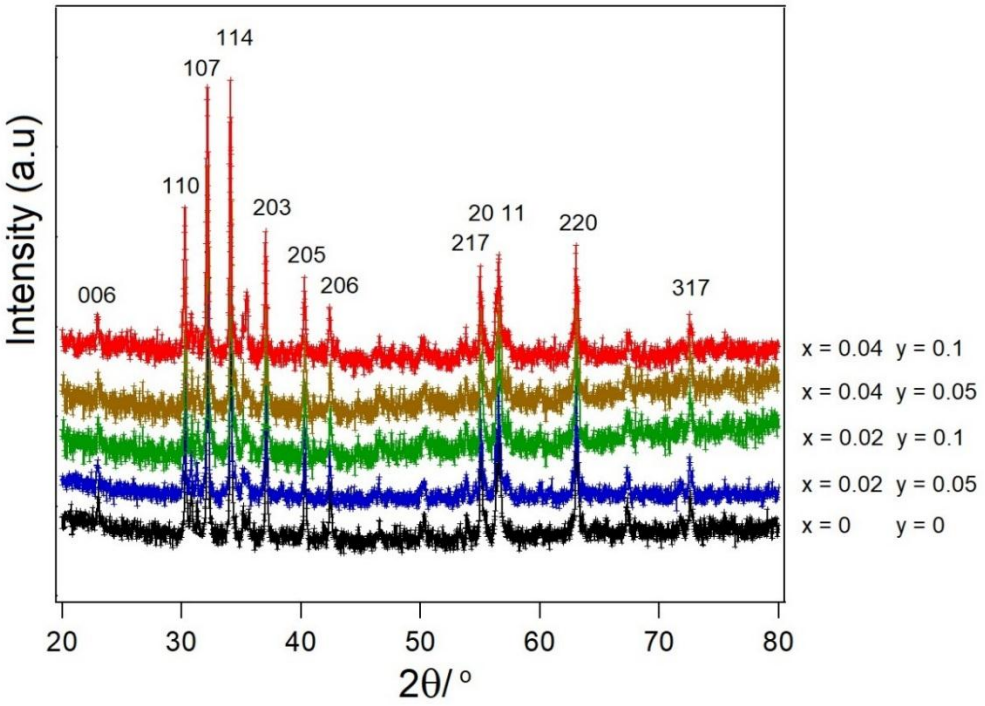

Figure 1. X-ray diffraction patterns $Ba_{1-x-y}La_xCe_yFe_{12}O_{19}$ (x = 0, 0.02, 0.04 and y = 0, 0.05, 0.1)

On the other hand, there appears to be a shift in Bragg diffraction peaks towards a large angle. This indicates a change in lattice parameters due to the presence of the La and Ce substitutions in the barium hexaferrite structure. While the reduced value of peak relative intensity with the increasing concentration of doping ions is thought to be related to the placement of crystallography sites in the crystal lattice due to the presence of doping ions (Fisher et al., 2016). A more quantitatively detailed analysis has been done using GSAS software so that it is known the structural parameters and crystallography site of each atom as presented in Figure 2.

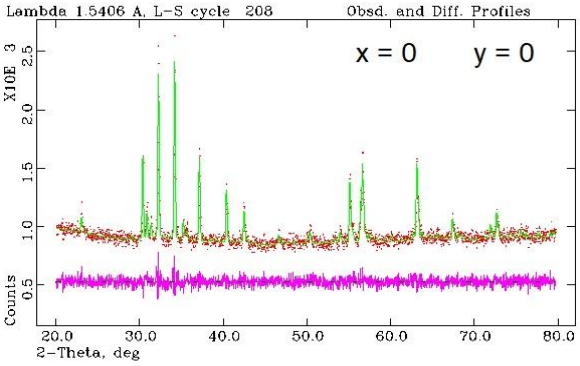

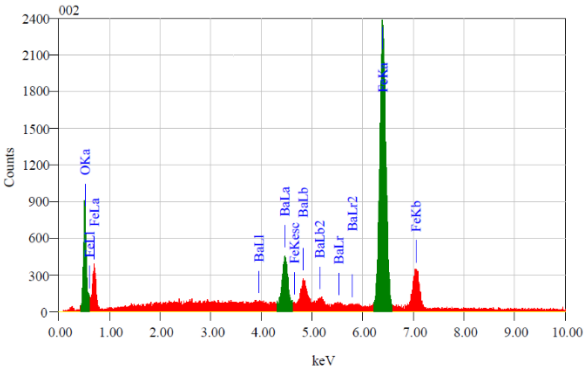

(a) x = 0 and y = 0

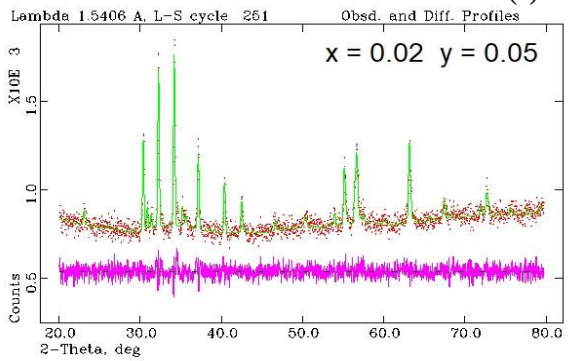

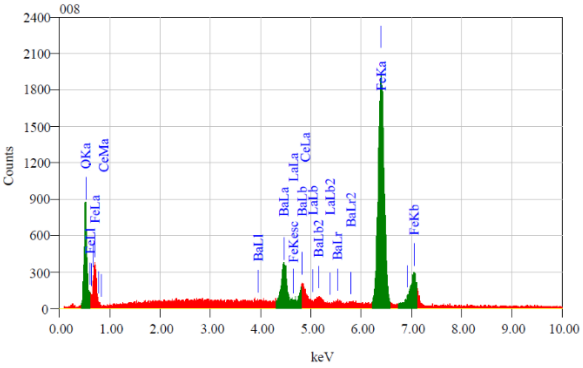

(b) x = 0.02 and y = 0.05

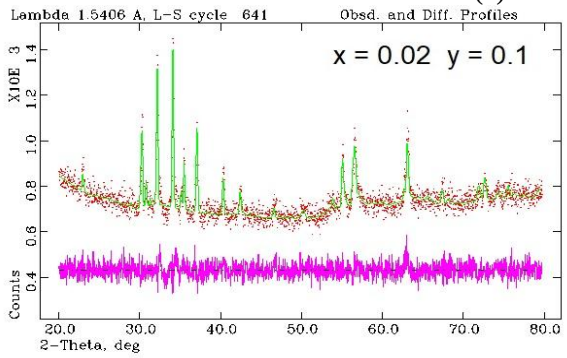

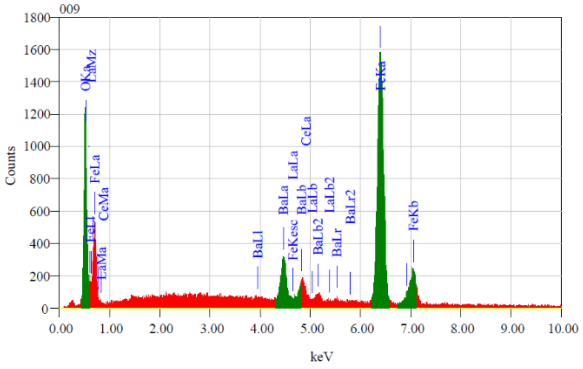

(c) x = 0.02 and y = 0.1

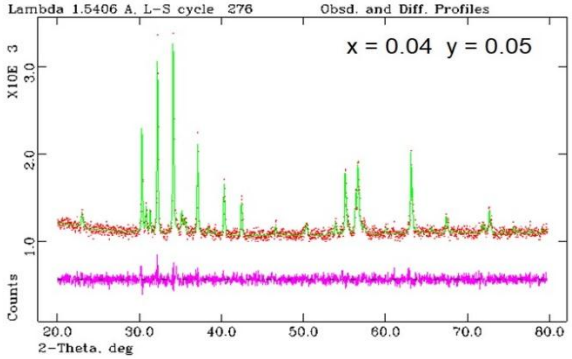

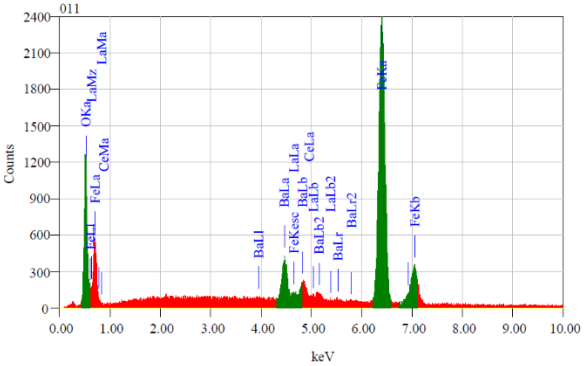

(d) x = 0.04 dan y = 0.05

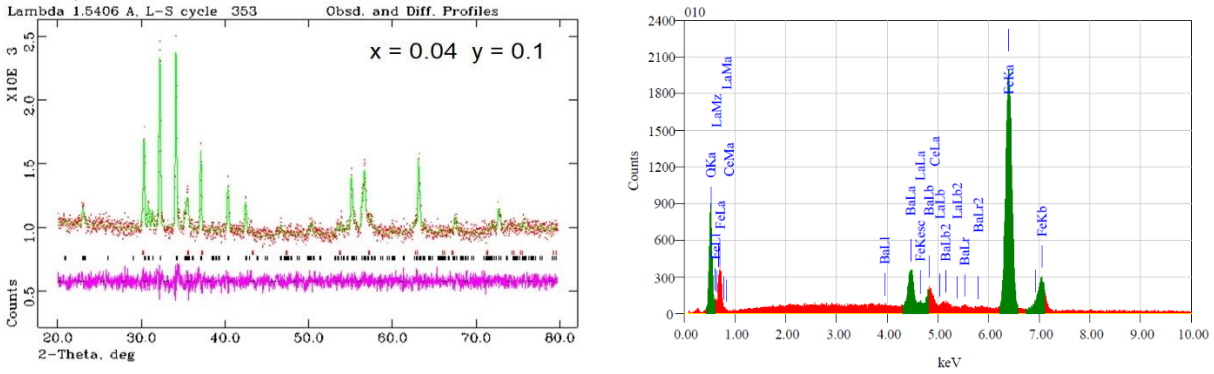

(e) x = 0.04 and y = 0.1

Figure 2. Refinement of X-ray diffraction patterns and EDS spectrum samples $Ba_{1-x-y}La_xCe_yFe_{12}O_{19}$

Barium hexaferrite has a hexagonal structure, of which Ba is a non-magnetic ion, while the carrier of magnetic properties is entirely determined only by the orbital momentum of the Fe^{3+} ion. All of the spin's magnetic moments are directed parallel to sites 2a, 2b, 12k while antiparallel spins are at sites 4f1 and 4f2 towards the c-axis. Substitutions of La and Ce occupy the position of the Ba^{2+} site so that Fe^{3+} was the main contributor responsible for magnetic properties, then after the appearance of Ce ions in the Ba site contributed also to its magnetic properties.

The success of this substitution is characterized by the emergence of doping elements that have been measured using energy dispersive spectroscopy (EDS). In the composition of $x > 0$ and $y > 0$, it is shown that in the sample has been detected elements La and Ce whose fraction is increasing along with the increasing concentration of doping ions. Table 1 is shown the parameters of the structure of quantitative analysis results of GSAS software that are fined with fitting parameters that have been following the required statistical standards, where Rwp < 10% and chi-squared $\chi^{(2)} < 1.3$.

Table 1
Parameters of the structure of the refinement pattern of X-ray diffraction patterns of $Ba_{1-x-y}La_xCe_yFe_{12}O_{19}$ consisting of lattice parameters, cell unit volume, atomic density, phase mass fraction formed

x	y	Phase	SG	R_{wp} (%)	χ^2	Lattice parameters (Å)				V (Å^3)	ρ (g/cm^3)
						a	b	c	c/a		
0	0	$BaFe_{12}O_{19}$	P 63/mmc	0.0362	1.230	5.884983	5.8951(3)	23.17972	3.939	695.231	5.726
0.02	0.05	$BaFe_{12}O_{19}$	P 63/mmc	0.0378	1.202	5.884483	5.8954(2)	23.16548	3.938	694.686	5.749
0.02	0.10	$BaFe_{12}O_{19}$	P 63/mmc	0.0404	1.221	5.884202	5.8956(3)	23.16114	3.936	694.49	5.743
0.04	0.05	$BaFe_{12}O_{19}$	P 63/mmc	3.18	1.218	5.88341	5.8968(4)	23.1591	3.936	694.241	5.755
0.04	0.10	$BaFe_{12}O_{19}$	P 63/mmc	3.43	1.211	5.88239	5.8971(3)	23.1517	3.935	693.779	5.751

Lattice parameters a, b, and c appear to decrease with increasing concentrations of La and Ce doping ions. This decrease in lattice parameters is due to the doping ion radius la (r = 145 pm) and Ce (r = 145 pm) being smaller than the radius of the atom Ba (r = 155 pm). So that the volume of cell units is also decreasing but in contrast to the atomic density that is seen increasing along with the increasing concentration of doping ions. The total atomic density is affected by the atomic density of the doping atom which is indeed much greater. In addition, the reduced value of this lattice parameter does not mean that the ferrite hexagonal structure is experiencing lattice distortion, but the barium hexaferrite structure still indicates the formation of a relatively stable structure. This can be proven from the ratio of changes in grid parameters c to a (c / a) which is still in the range of 3.93 - 3.94. This ratio is a validation of the formation of an M-type hexagonal structure.

Conclusion

The synthesis of samples $Ba_{1-x-y}La_xCe_yFe_{12}O_{19}$ (x = 0, 0.02, 0.04 and y = 0, 0.05, 0.1) has been successfully done using the wet mechanical milling method. X-ray diffraction pattern measurements showed that all samples had a single phase of barium hexaferrite with an M-type hexagonal structure. The lattice parameter decreases with the increasing concentration of La^{3+} and Ce^{4+} ions.

References

Adnyana, I. G. A. P., Suarbawa, K. N., Adi, W. A., Wardani, N. N. S. K., & Jalut, L. L. S. (2019). The Effect of Lanthanum Substitution on the Coercivity Field in Oxide Permanent Magnet Based on Ba1-xLaxFe12O19:(X= 0; 0.02; 0.04; and 0.08). *International journal of physical sciences and engineering*, *3*(1), 42-49.

Adnyana, I. G. A. P., Sukarasa, I. K., & Adi, W. A. (2020). Rare earth ion contribution in barium hexaferrite structure to a change of magnetocrystalline anisotropy to improving its magnetic properties. *International Journal of Physical Sciences and Engineering*, *4*(2), 1-13.

Bahadur, A., Saeed, A., Iqbal, S., Shoaib, M., Ahmad, I., ur Rahman, M. S., ... & Hussain, W. (2017). Morphological and magnetic properties of BaFe12O19 nanoferrite: A promising microwave absorbing material. *Ceramics International*, *43*(9), 7346-7350. https://doi.org/10.1016/j.ceramint.2017.03.039

El Shater, R. E., El-Ghazzawy, E. H., & El-Nimr, M. K. (2018). Study of the sintering temperature and the sintering time period effects on the structural and magnetic properties of M-type hexaferrite BaFe12O19. *Journal of Alloys and Compounds*, *739*, 327-334. https://doi.org/10.1016/j.jallcom.2017.12.228

Fisher, J. G., Sun, H., Kook, Y. G., Kim, J. S., & Le, P. G. (2016). Growth of single crystals of BaFe12O19 by solid state crystal growth. *Journal of Magnetism and Magnetic Materials*, *416*, 384-390. https://doi.org/10.1016/j.jmmm.2016.04.079

Haritsah, I., Adi, W. A., Purwani, M. V., & Manaf, A. (2019, March). Improved separation of Ce, La, and Nd from a concentrate of rare-earth hydroxide via fractional precipitation. In *IOP Conference Series: Materials Science and Engineering* (Vol. 496, No. 1, p. 012013). IOP Publishing.

Li, R., Pang, S., Ma, C., & Zhang, T. (2007). Influence of similar atom substitution on glass formation in (La–Ce)–Al–Co bulk metallic glasses. *Acta Materialia*, *55*(11), 3719-3726. https://doi.org/10.1016/j.actamat.2007.02.026

Mosleh, Z., Kameli, P., Ranjbar, M., & Salamati, H. (2014). Effect of annealing temperature on structural and magnetic properties of BaFe12O19 hexaferrite nanoparticles. *Ceramics International*, *40*(5), 7279-7284. https://doi.org/10.1016/j.ceramint.2013.12.068

Nonaka, T., Ohbayashi, G., Toriumi, Y., Mori, Y., & Hashimoto, H. (2000). Crystal structure of GeTe and Ge2Sb2Te5 meta-stable phase. *Thin Solid Films*, *370*(1-2), 258-261. https://doi.org/10.1016/S0040-6090(99)01090-1

Rezlescu, L., Rezlescu, E., Popa, P. D., & Rezlescu, N. (1999). Fine barium hexaferrite powder prepared by the crystallisation of glass. *Journal of Magnetism and Magnetic Materials*, *193*(1-3), 288-290. https://doi.org/10.1016/S0304-8853(98)00442-9

Song, X., Wang, Y., An, C., Guo, X., & Li, F. (2008). Dependence of particle morphology and size on the mechanical sensitivity and thermal stability of octahydro-1, 3, 5, 7-tetranitro-1, 3, 5, 7-tetrazocine. *Journal of hazardous materials*, *159*(2-3), 222-229. https://doi.org/10.1016/j.jhazmat.2008.02.009

Vinnik, D. A., Chernukha, A. S., Gudkova, S. A., Zhivulin, V. E., Trofimov, E. A., Tarasova, A. Y., ... & Niewa, R. (2018). Morphology and magnetic properties of pressed barium hexaferrite BaFe12O19 materials. *Journal of Magnetism and Magnetic Materials*, *459*, 131-135. https://doi.org/10.1016/j.jmmm.2017.11.085

Xu, X., Wen, Z., Yang, X., Zhang, J., & Gu, Z. (2006). High lithium ion conductivity glass-ceramics in Li2O–Al2O3–TiO2–P2O5 from nanoscaled glassy powders by mechanical milling. *Solid State Ionics*, *177*(26-32), 2611-2615. https://doi.org/10.1016/j.ssi.2006.04.010